# Quantum sensor for atom-surface interactions below 10 $\mu$m

F. Sorrentino, A. Alberti, G. Ferrari, V. V. Ivanov, N. Poli, M. Schioppo, and G. M. Tino*
*Dipartimento di Fisica and LENS, Università di Firenze, INFN Sezione di Firenze, CNR-INFM, via Sansone 1, 50019 Sesto Fiorentino, Italy*

(Received 30 October 2008; published 9 January 2009)

We report the realization of a quantum device for force sensing at the micrometric scale. We trap an ultracold $^{88}$Sr atomic cloud with a one-dimensional (1D) optical lattice; then we place the atomic sample close to a test surface using the same optical lattice as an elevator. We demonstrate precise positioning of the sample at the micrometer scale. By observing the Bloch oscillations of atoms into the 1D optical standing wave, we are able to measure the total force on the atoms along the lattice axis, with a spatial resolution of few micrometers. We also demonstrate a technique for transverse displacement of the atoms, allowing us to perform measurements near either transparent or reflective test surfaces. In order to reduce the minimum distance from the surface, we compress the longitudinal size of the atomic sample by means of an optical tweezer. This system is suited for studies of atom-surface interaction at short distance, such as measurement of the Casimir force and the search for possible non-Newtonian gravity effects.

DOI: 10.1103/PhysRevA.79.013409 PACS number(s): 37.10.Gh, 81.16.Ta, 07.07.Df

## I. INTRODUCTION

The use of ultracold atoms for studying forces at small length scales has been recently addressed by several groups, both experimentally [1,2] and theoretically [3,4]. Besides the technological implications [5], measuring forces at short distances has become attractive for several research fields in physics, from the Casimir effect [1] to possible violations of Newtonian gravity [6,7].

Force sensing at the submillimeter scale has been achieved with several techniques based on the interaction between mesoscopic objects [8–14]. Ultracold atoms offer additional degrees of freedom, and provide a new class of sensors combining good accuracy with high spatial resolution. For instance, by measuring the radial oscillation frequency of a Bose-Einstein condensate in a magnetic trap it is possible to detect forces as weak as $\sim 10^{-4}$ times the earth gravity, such as the atom-surface (Casimir-Polder) force at distances lower than $\sim 8$ $\mu$m [1,15]. Higher sensitivity is expected from the use of atom interferometry [3,16–18]. A promising technique consists in observing the Bloch oscillations of the atomic momentum in a one-dimensional (1D) optical lattice [19]. The oscillation frequency $\nu_B$ is simply related to the force $F$ acting on the atoms along the lattice axis:

$$\nu_B = \frac{F\lambda_L}{2h}, \tag{1}$$

where $\lambda_L$ is the wavelength of the light producing the lattice, and $h$ is Planck's constant.

Most of the proposed schemes make use of quantum degenerate gases. One major advantage of this approach is the very small momentum spread of atomic samples at ultralow temperatures where quantum degeneracy occurs. On the other hand, the effect of interatomic collisions at high density may be detrimental to precision measurements, causing uncontrollable phase shift or decoherence of the quantum degrees of freedom under analysis. A strong suppression of binary collisions occurs in spin-polarized degenerate Fermi gases [20]; however, in such systems the lowest possible temperature is limited by Fermi pressure. Better performance is expected from the use of Bose-Einstein condensates: a similar effect of collision suppression can be obtained in a Bose gas, using Feshbach resonances to tune the interatomic cross section [21,22].

We adopted a different approach. In two recent papers we demonstrated that excellent performances can be obtained using a classical ultracold gas, by choosing atoms with suitable properties [2,23]. In this respect, $^{88}$Sr represents an ideal candidate for precise quantum sensors, as it combines low sensitivity to magnetic fields with remarkably small atom-atom interactions [24,25]. Moreover, the absence of orbital, electronic, and nuclear angular momentum is of great importance for measurements close to solid surfaces, as it makes the atom immune from rf fields [26]. These are a source of decoherence in most of the other schemes, by inducing spin-flip transitions and subsequent collisional relaxation in spin-polarized fermionic samples, or by interfering with Feshbach resonances in degenerate Bose gases.

In this paper we describe the all-optical implementation of a quantum sensor for accurate force measurements with high spatial resolution, based on a sample of ultracold strontium atoms. By means of laser manipulation techniques, we can place an ultracold $^{88}$Sr sample close to a test surface. The coherence of Bloch oscillations is preserved in the vicinity of the surface, and the atom-surface interaction can be detected through a shift in the oscillation frequency.

Our sensor can be employed to study the Casimir-Polder force at the crossover to the thermal regime [1,15], and to search for possible deviations from Newtonian gravity below 10 $\mu$m. For this purpose we employ a suitable test surface with both transparent and metal-coated regions. An optical elevator brings the sample close to the transparent part of the surface, and we developed a technique for moving the atomic sample along the surface by several millimeters; in particular, we can transfer the atoms onto the metal-coated region of the test surface, where short-distance gravity tests

*guglielmo.tino@fi.infn.it

 

can be performed. Moreover, using an optical tweezer we compress the size of our $^{88}$Sr sample to a few micrometers along the direction orthogonal to the test surface; this allows us to approach the range of atom-surface distance below 10 $\mu$m.

## II. GENERAL SCHEME

In order to perform force measurements at small length scale, three main tasks are to be undertaken; i.e., one needs a proper test surface, then a probe of very small size to be precisely positioned at a short distance from it, and a suitable readout technique to detect the interaction between the probe and the test surface.

In our work the probe is represented by a sample of ultracold strontium atoms trapped in an optical lattice. The basic idea for our small-distance force sensor is to employ an optical elevator (see Sec. III) to place the atomic sample close to the test surface. The atomic wave function evolution within the periodic potential of the optical lattice provides a technique to read out atom-surface interactions (see Sec. IV).

The optical elevator requires independent control of the optical phase of the two counterpropagating lattice laser beams. Clearly, such a scheme for sample positioning at micrometric distances limits the choice of test surface to transparent materials. However, a precise positioning close to metallic surfaces may be desirable as well. This is the case when studying gravitational interactions at short distance: the unavoidable atom-surface electromagnetic interactions become dominant at distance of a few micrometers, even with dielectric substrates; the best approach to detect tiny gravitational forces is then to shield electrodynamic effects with a thin metal layer [10].

We developed a more general positioning technique allowing also for measurements close to a metallic surface. Our method benefits from the effect of residual surface reflectivity discussed in Sec. III, and is described in Fig. 1. The basic idea is to employ a test surface made of a glass plate which is rigidly connected to a test mass of composite structure—i.e., made of alternating regions of two different materials such as Au and Al, having a high density contrast but similar electric and thermal properties, in order to generate a purely gravitational alternating potential. The test mass is coated with a "Casimir shield," i.e., a gold layer with a thickness of ~500 nm, which is larger than the plasma length (130 nm in gold) but smaller than the length scale to be explored with the force sensor (1–10 $\mu$m). The surface of the glass plate close to the test mass has a gradient gold coating whose depth smoothly rises from zero to the thickness of the Casimir shield. We first place the atoms close to the transparent part of the test surface, using the optical elevator; then we trap the atoms in the shallow standing wave provided by a single reflected laser beam; finally, we translate the atoms across the surface at constant distance from it, by moving the lattice beam transversely.

We start the sensor preparation from a submicrokelvin atomic sample in a magneto-optical trap (MOT). The process of cooling and trapping strontium atoms below the photon recoil limit has been described in detail elsewhere [27–29]; it

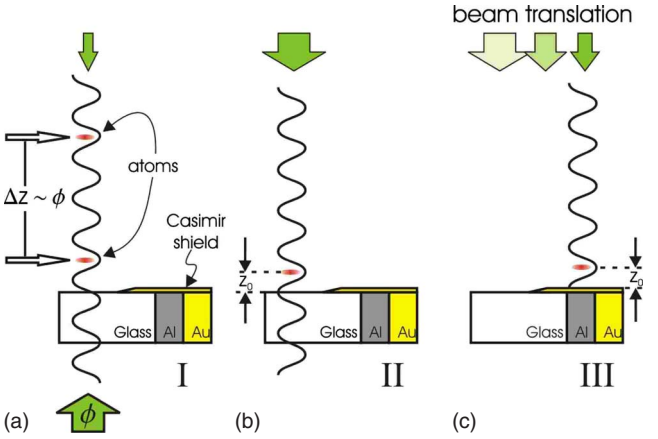


FIG. 1. (Color online) Illustration of the positioning technique: (a) the atoms are first placed close to the transparent part of the test surface; (b) then the counterpropagating lattice beam is switched off adiabatically, and the atoms remain trapped in the standing wave made of the copropagating beam and the weak reflected beam; (c) the lattice beam is translated laterally through the region with varying metal coating, and the atoms are placed close to the Casimir shield. The width of the arrows represents the relative intensity of laser beams. A simplified version of the test surface, made of a glass plate with a gold-shaded coating is shown in Fig. 7 and has been used for the tests described in Sec. V.

consists in a double-stage magneto-optical trapping scheme: a "blue MOT" operated on the $^1S_0-^1P_1$ transition at 461 nm, with an atomic temperature of few millikelvin, followed by a "red MOT" operated on the $^1S_0-^3P_1$ intercombination transition at 689 nm, where the minimum attainable temperature is approximately half the photon recoil limit, i.e., 230 nK. In the final red MOT the shape of the atomic cloud is rather flat, as the atoms sag on the bottom of the ellipsoidal shell where they are in resonance with the Zeeman-shifted laser field in the MOT magnetic quadrupole [28]. The vertical size of the atomic cloud is basically limited by the linewidth of the cooling transition. After trapping them into the red MOT we transfer the atoms to a vertical 1D optical lattice. The standing wave is produced with two counterpropagating laser beams. As reported in Ref. [2], when directly transferring the atoms from the red MOT to a vertical optical lattice, we obtain a disk-shaped sample with a rms vertical halfwidth of ~12 $\mu$m and a horizontal radius of ~150 $\mu$m. Typical atomic population and temperature in the lattice are $10^5$ atoms and 400 nK. We observe Bloch oscillations of the vertical atomic momentum by releasing the optical lattice at a variable delay, and by imaging the atomic distribution after a fixed time of free fall. We measure a coherence time for the Bloch oscillation of 12 s, corresponding to ~7000 oscillations. These values are among the highest ever observed for Bloch oscillations in atomic systems [21]. Measuring the oscillation frequency, we determine the vertical force on the atoms—namely, the earth's gravity—with a resolution of $5\times10^{-6}$. Even better resolution can be attained by means of coherent delocalization of the atomic wave packet, as reported in [23] where the earth's gravity was measured with a precision of $2\times10^{-6}$.

The optical lattice beams are generated by a single-mode 532 nm $Nd:YVO_4$ laser with an overall output power of

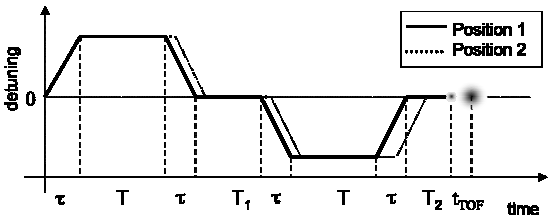


FIG. 2. Temporal sequence for the atom positioning at different distances from the surface using the optical elevator. To change the minimum atom-surface distance we vary the time $T$ of uniform motion; we change the time $T_2$ correspondingly to keep the overall trapping time in the lattice, $T_{\mathrm{trap}}=4\tau+2T+T_1+T_2$, constant. We vary the time $T_1$ to observe Bloch oscillations.

5 W. At the chosen laser wavelength, the photon scattering rate causes negligible heating, while the photon recoil is high enough for clear observation of Bloch oscillations [2]. The optical power ratio between the two beams can be tuned by means of a half-wave plate mounted on a motorized rotation stage before a polarizing beam splitter. We have independent AM and FM control on the two beams by means of two acousto-optical modulators (AOMs) used in single-pass geometry. The rf signals driving the two AOMs are synthesized from the same stable 400 MHz oscillator. Each beam is coupled into a single-mode optical fiber after the AOM, to avoid misalignment at the trap position during the AOM frequency tuning. Both beams are weakly focused on the atoms, with a waist of $\sim$200 $\mu$m.

### III. OPTICAL ELEVATOR

The optical lattice has a double use: it provides the periodic potential where Bloch oscillations occur, and at the same time it serves as an elevator for accurately positioning the sample close to a transparent surface. We translate the atomic sample along the lattice axis by giving a relative frequency offset to the laser beams [30,31]. We typically apply a linear frequency ramp to one AOM for a time $\tau$, up to a frequency difference $\delta\nu$. We then keep the frequency difference constant for a time $T$, and we finally stop the atoms by bringing the frequency difference back to zero with a linear ramp of duration $\tau$. The overall vertical displacement is then $\Delta z=\frac{1}{2}\lambda\delta\nu(\tau+T)$, where $\lambda$ is the wavelength of the lattice beams. This can also be expressed as $\Delta z=(\lambda/4\pi)\phi$, where $\phi$ is the relative optical phase accumulated between the two beams (see Fig. 1). By varying only the duration $T$ of the uniform motion, we change the vertical displacement without affecting the overall momentum transferred to the atoms by the elevator. The whole sequence is illustrated in Fig. 2. We keep the frequency chirp of the lattice beam low enough to avoid additional trap losses in the acceleration phase [32]: typical acceleration is of the order of $g$.

In this way we can place the atoms close to a transparent test surface. The surface is located $\sim$5 cm below the MOT region. We measure the number of atoms and the phase of the Bloch oscillation with absorption imaging after bringing the atoms back to the original position. This is done by applying to the other AOM a frequency shift with the same

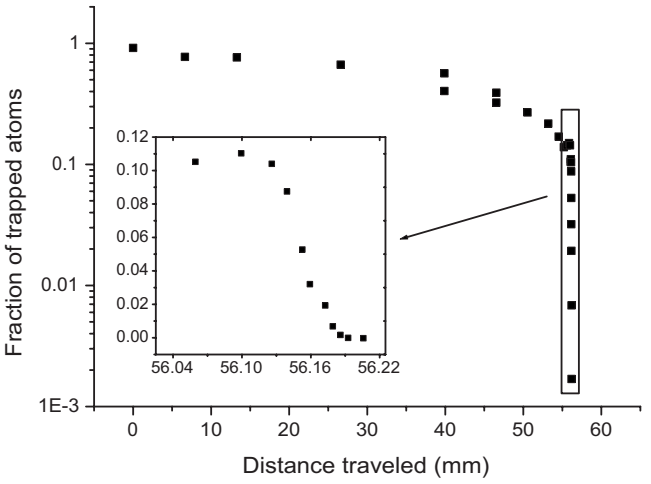


FIG. 3. Fraction of atoms recorded after the elevator round trip, versus vertical displacement. The inset shows the region close to the test surface. The vertical displacement is varied by changing the duration of the motion at uniform velocity, but the number of atoms is always measured at the same delay after the transfer from the MOT.

temporal scheme as described above. In Fig. 3 we show the number of atoms recorded after an elevator round trip, as a function of the distance $\Delta z$. A sudden drop, corresponding to the loss of atoms kicking the test surface, is clearly visible. The plot gives a direct measure of the vertical size of the atomic sample. By fitting the curve in the inset with an Erf function we obtain the $1/e^2$ halfwidth $\delta z$. The resulting value of $\sim$13 $\mu$m is in agreement with *in situ* imaging of the atomic spatial distribution.

When studying atom-surface interactions in the presence of strongly distance-dependent effects, as in the case of the Casimir-Polder force, one key point is the precision of sample positioning close to the surface. A possible source of instability in the atom displacement is the elevator itself, so we measured the fluctuations in the vertical position before and after the sample round trip, through *in situ* absorption imaging. The results are shown in Fig. 4(c): The measured 3 $\mu$m statistical uncertainty on the vertical position is mainly

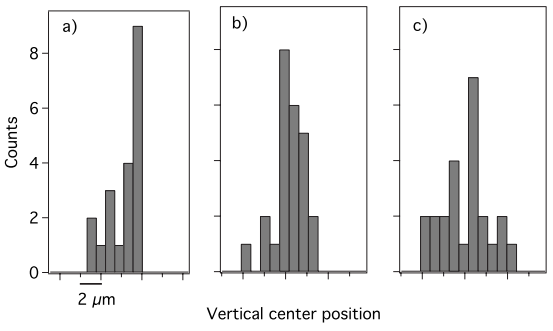


FIG. 4. Distribution of the sample mean vertical position as measured from the absorption images before (a) and (c) and after (b) the elevator round trip. In (a) and (b) an optical tweezer was employed to shrink the vertical cloud size (see below), while in (c) the atoms were transferred to the optical lattice directly from the MOT.

due to the width of the atomic distribution and to fluctuations in the red laser frequency or in the MOT magnetic field. Figure 4 also reports a similar measurement with the use of an optical tweezer to reduce the vertical size of the sample (see below). In this case the statistical uncertainty on the vertical position is 2 $\mu$m either with or without the elevator round trip, and is basically limited by the resolution of our imaging system, showing that the elevator does not introduce additional fluctuations at this level.

In order to optimize the transfer efficiency of atoms close to the test surface, we studied the possible mechanisms of atom losses along the operation of the optical elevator. Typical losses, as can be seen from the slow decay in Fig. 3 before the sudden drop shown in the inset, cannot be explained in terms of background gas collisions, since the trap lifetime is of the order of a few seconds while the typical duration of the elevator round trip is a few hundreds of milliseconds. By varying the frequency chirp on the AOMs by one order of magnitude we did not observe significant changes in the transfer efficiency. This rules out the effect of lattice acceleration on the excess losses. Changes in the trap depth due to the divergence of the laser beams is not likely to limit the effective trap lifetime to such an extent, as the Rayleigh length is larger than the overall atom displacement. In fact, we observed that axially shifting the waist position of both laser beams by several centimeters does not seriously affect the amount of additional losses. Instead we found that the round-trip transfer efficiency of the elevator strongly depends on the intensity ratio between the lattice laser beams. We ascribe the observed losses to the excitation caused by the reflectivity of the test surface.

For clarity, throughout the text we will refer to the lattice beam propagating in the vacuum cell toward the test surface, which is oriented downward in Fig. 1, as the "copropagating" beam; we refer to the other lattice beam, which is oriented upward in Fig. 1, as "counterpropagating." The interference between the copropagating beam and the reflected beam causes a fast modulation in the shape of the optical potential during the operation of the elevator. Lowering the intensity of the copropagating beam reduces this effect, but makes the lattice trap shallower. As shown in Fig. 5, the fraction of residual atoms is maximum when the beam propagating toward the test surface is less intense than the other one by a factor of $\sim$25. The optimal power ratio obviously depends on the surface reflectivity, which is $R \sim 8\%$ in our case. Such relatively high reflectivity is important for our positioning scheme, as described in Sec. V. However, the effect just described might be non negligible even with an antireflection coating on the test surface. In fact, if we indicate by $E_{\mathrm{down}}$ the amplitude of the copropagating wave, by $E_{\mathrm{up}}$ the amplitude of the counterpropagating wave, and by $E_{\mathrm{refl}}=\sqrt{R}E_{\mathrm{down}}$ the amplitude of the reflected wave, the lattice potential depth is $U=\mathrm{const}\times E_{\mathrm{down}}E_{\mathrm{up}}$ while the interference between $E_{\mathrm{down}}$ and $E_{\mathrm{refl}}$ produces a modulation depth $\delta U = 2\times \mathrm{const}\times E_{\mathrm{down}}E_{\mathrm{refl}}$. Thus the ratio of the spurious modulation and the trap depth is

$$\frac{\delta U}{U} = 2\sqrt{R}\frac{E_{\mathrm{down}}}{E_{\mathrm{up}}}. \tag{2}$$

For $E_{\mathrm{down}} \simeq E_{\mathrm{up}}$, even with a residual window reflectivity as low as $R \sim 0.1\%$, this ratio would be higher than 6%. In the reference frame of the moving atoms, the lattice potential is modulated at a frequency $v/\lambda$, where $v$ is the velocity of the elevator. In any case, provided the ratio $E_{\mathrm{down}}/E_{\mathrm{up}}$ is sufficiently low, the additional losses are not detrimental to the sensor operation. As shown in Fig. 5, with the optimal power ratio we obtain 20% transfer efficiency throughout the elevator round trip. For lower values of the power ratio the lattice trap becomes too shallow, thus reducing the transfer efficiency. It should be remarked that the optimal efficiency depends on surface reflectivity. Using a different test surface with reflectivity of 1%, we achieved up to 50% efficiency

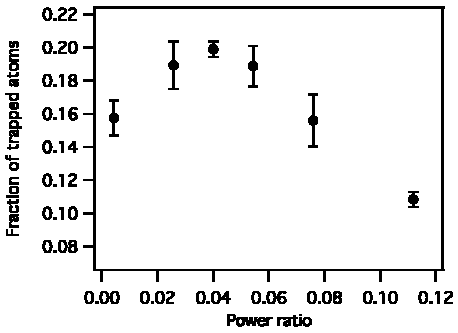


FIG. 5. Fraction of residual trapped atoms after the optical elevator round trip vs copropagating to counterpropagating beam power ratio. The overall optical power in the lattice beams is kept constant. In this measurement the atoms are brought to a minimum distance of $\sim$100 $\mu$m from the surface, so that losses due to direct atom-surface collision are negligible.

In principle, the lattice modulation could also affect the momentum distribution along the lattice axis. Anyway, we found that the sample temperature is not seriously perturbed by operating the elevator up to a velocity of 20 m/s. We also checked that in our experimental conditions this effect gives no appreciable decoherence of Bloch oscillations; instead we found that residual lattice modulation causes a position-dependent phase shift in the Bloch oscillations. However, the position-dependent phase shift is highly reproducible, allowing an unambiguous measurement of the Bloch frequency at any given atom-surface displacement.

## IV. BLOCH OSCILLATIONS

To detect the atom-surface interaction we move the sample close to the surface with the sequence described above (constant acceleration for time $\tau$, uniform motion for time $T$, constant deceleration for time $\tau$), then we keep it still for a variable time $T_1$, bring it back with an inverted sequence, and keep it still in the starting position for a time $T_2$ before releasing the trap for absorption imaging (see Fig. 2). We measure the phase of the Bloch oscillation through the width of the vertical momentum-space distribution [2], by imaging the atoms after a fixed time $t_{\mathrm{TOF}}$ of free fall. Increasing $t_{\mathrm{TOF}}$ gives improved resolution in the momentum distribution mapping, but it reduces the atomic density and thus the signal-to-noise ratio on the charge-coupled device camera for absorption imaging. We compensate for this effect by switching off one single lattice beam in the time-of-flight (TOF) measurement, thus preventing radial expansion of the

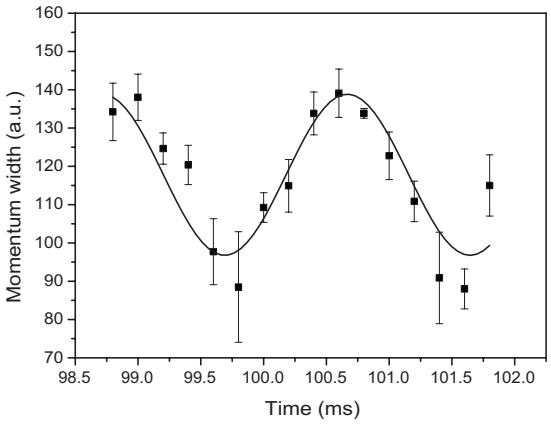


FIG. 6. Bloch oscillations of the atomic momentum measured with atoms at a distance of 15 $\mu$m from the test surface; each point represents the average of three values of the momentum width; error bars are given by statistical uncertainty; the solid curve is a sinusoidal fit to the data; the horizontal coordinate is the time $T_1$ as shown in Fig. 2.

atomic cloud. In this way we can set $t_{\mathrm{TOF}}=12$ ms and still be able to detect the Bloch oscillations with as few as $10^3$ atoms. To observe the Bloch oscillations we vary the time $T_1$.

The detected phase $\phi$ of the Bloch oscillation is proportional to the overall momentum transferred to the atoms in the trapping time $T_{\mathrm{trap}}=4\tau+2T+T_1+T_2$:

$$\phi = \int_0^{T_{\mathrm{trap}}} [F(z) - ma(t)] \frac{\lambda_L}{2h} dt \tag{3}$$

where $F(z)$ is the force along the lattice axis and $a(t)$ is the acceleration. We change the atom-surface separation by varying the time $T$, and we vary the time $T_2$ correspondingly so to keep the whole duration $T_{\mathrm{trap}}$ constant. In this way, in the absence of extra lattice modulation due to the residual reflectivity of the upper window, we would expect the phase $\phi$ to be constant for small and fixed values of $T_1$. In fact no net extra momentum is transferred through the lattice acceleration, and the impulse of the force gradients is negligible for small $T_1$.

The Bloch frequency at a given atom-surface displacement is measured by recording a few oscillations at short ($T_1 \sim 0-10$ ms) and at long evolution times ($T_1 \sim 1$ s in this experiment). We also sample a few oscillation periods at intermediate times to avoid aliasing and to rule out a possible chirp of the Bloch frequency due to spurious effects [1].

Typical recorded data for atom-surface distance of 15 $\mu$m are shown in Fig. 6. Bloch oscillations can be clearly observed in such conditions, even if the tail of the atomic distribution is cut by the test surface.

By changing the atom-surface displacement up to a minimum value of $\sim 15$ $\mu$m we do not observe any shift in the frequency of Bloch oscillations with 1 s of measurement time, showing that the position-dependent phase shift does not alter the force measurement with this scheme. This is consistent with the magnitude of the expected atom-surface interactions. The asymptotic behavior of the Casimir-Polder force in the thermal regime, that is, for distances higher than the thermal wavelength $\lambda_T=\hbar c/k_B T$, is described by [33,34]

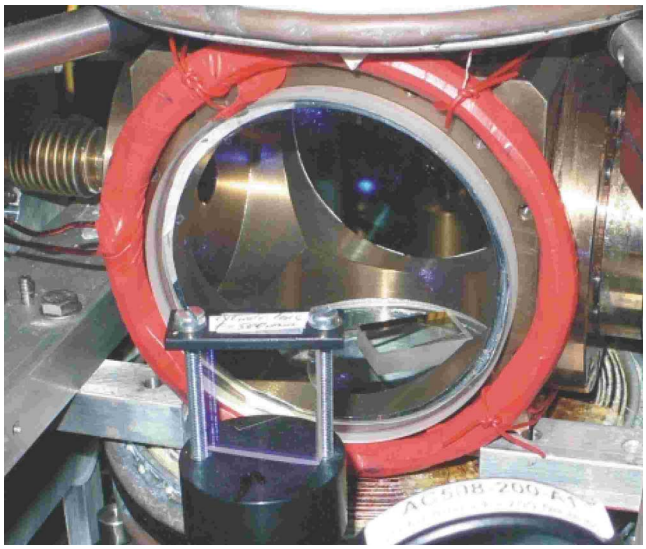

FIG. 7. (Color online) Picture of the vacuum chamber; the test surface is placed on the lower window; at the cell center, the atomic cloud in the blue MOT is also visible.

$$F_{\mathrm{therm}} = \frac{3\alpha_0 k_B T}{4d^4} \frac{\epsilon_0 - 1}{\epsilon_0 + 1} \tag{4}$$

where $\alpha_0$ and $\epsilon_0$ are the dc atomic polarizability and the dielectric constant of the test surface, respectively, while $d$ is the atom-surface distance. The magnitude of such a force at $d=15$ $\mu$m can be computed as $0.7\times10^{-6}$ mg using $\alpha_0 = 2.77\times10^{-23}$ cm$^3$ [35] and $\epsilon_0=3.4$. With the available signal-to-noise ratio we are sensitive to a phase shift of $\sim 0.08$ rad; such a shift would be caused by a force of $\sim 2\times10^{-5}$ mg after 600 oscillations, that is, after 1 s.

Observation of the frequency of Bloch oscillations is not the only possible readout technique for atom-surface interactions. As already shown in [23,36], even more sensitive force measurements may be attained by means of coherent delocalization of the atomic wave packet in the optical lattice.

## V. TRANSVERSE TRANSLATION

In order to demonstrate our positioning method illustrated in Fig. 1, we put into the MOT vacuum cell a simple test surface made of a SF6 glass plate with an uncoated region as well as a region of gold-shaded coating (Fig. 7). As a first step we transfer the atomic sample close to the uncoated part of the test surface using our elevator, as described above. Then we trap the atoms in the shallow optical lattice generated by the copropagating laser field and the reflected field. For this purpose we extinguish the counterpropagating lattice beam adiabatically by rotating the half-wave plate before the polarizing beam splitter that generates the two lattice beams. In order to maximize the number of trapped atoms at this stage, we keep the intensity of the copropagating beam low during the elevator, as discussed above; then we increase it to maximize the final trap depth. In this way we can transfer

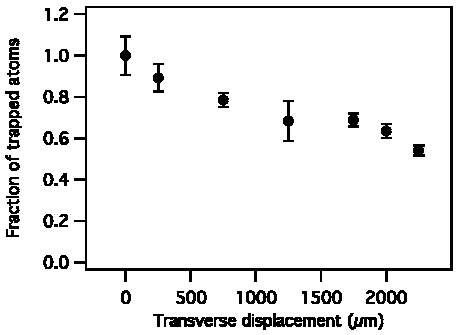


FIG. 8. Fraction of residual trapped atoms after transverse translation, versus the distance traveled along the surface. Maximum acceleration is 2 $mm/s^2$.

nearly 50% of the atoms into the retroreflected-beam trap.

As a final step, we translate the atoms along the test surface by moving the lattice laser beam transversely. The output coupler of the optical fiber delivering the copropagating beam as well as the focusing lens are mounted on a motorized translation stage. The translation axis is orthogonal to the beam propagation direction. The transverse acceleration is kept as low as 2 $mm/s^2$ to limit loss of atoms because of the soft radial frequency of the optical trap.

Figure 8 shows the number of residual trapped atoms after the transverse displacement, versus the distance traveled. In 4 s the atoms travel more than 2 mm forth and back along the surface, reaching the gold-shaded coating. A major contribution to the ~50% losses in Fig. 8 is given by background collisions.

## VI. SAMPLE COMPRESSION WITH OPTICAL TWEEZERS

The disk-shaped geometry of our sample is suited for force measurements close to a horizontal surface. However, the minimum attainable atom-surface distance is limited by the vertical size of the atomic distribution. In particular, to measure the force between 5 and 10 $\mu$m from the surface, we should compress our sample by at least a factor of 3 in the vertical direction. For this purpose we employ an optical tweezer, made of a far-off resonant optical dipole trap (FORT). This is obtained with a strongly astigmatic laser beam with the vertical focus centered on the atoms. In that position the $1/e^2$ halfwidth of the laser beam is ~10 $\mu$m in the vertical direction, and can be easily varied between 1 and 3 mm in the horizontal direction by moving a cylindrical lens. Laser power and wavelength are 8 W and 1064 nm, respectively.

We transfer the atoms into the FORT by superposing the laser beam to the atoms in the final red MOT stage. We attain a rather high transfer efficiency of ~50% due to the large spatial overlap between the two traps. The optical trap gives a very weak confinement in the tranverse horizontal direction, where the atoms quickly diffuse after the red MOT is switched off. Figure 9 shows an absorption image taken 10 ms after switching off the red MOT. The vertical size of the atomic sample in the optical tweezer is smaller than the

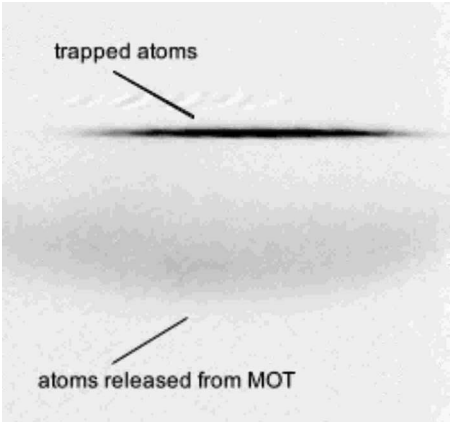


FIG. 9. Absorption image of the atoms 8 ms after swiching the red MOT off. Below the atoms trapped into the optical tweezer, the untrapped atoms in free fall are visible.

resolution of our imaging system. We deduce the rms vertical halfwidth $\sigma_z$ by measuring the vertical trap frequency $\omega_z$ and the vertical atomic temperature $T_z$, and then using

$$\sigma_z = \sqrt{\frac{k_B T_z}{m\omega_z^2}} \tag{5}$$

where $k_B$ is the Boltzmann constant and $m$ is the atomic mass. The measured vertical temperature slightly decreases in the first 20 ms, as the atoms diffuse horizontally. The value of $\sigma_z$ ranges between 3 and 4 $\mu$m, depending on the position of the cylindrical lens and the diffusion time of the atoms in the horizontal direction. Better vertical confinement might be achieved either by tighter focusing of the optical tweezer beam, or through more complex optical configurations such as using Hermite-Gaussian beams [37].

After shrinking the vertical size of the atomic cloud with the optical tweezer, we trap the sample into the optical lattice and we move the atoms close to the surface using the elevator. The transfer efficiency from the optical tweezer to the lattice is mainly limited by the geometrical overlap between the two traps and by the ratio of atomic temperature and lattice trap depth. Typical values are in the range ~15%.

The vertical size of the atomic sample after transfer from tweezer to lattice can be measured with the technique described in Fig. 3; we measured a width of about 8 $\mu$m rms. The resulting size critically depends on a number of experimental parameters, such as the trap depth in the tweezer and in the lattice, the sample temperature, and the time scale over which the transfer occurs. We expect that, after careful optimization, the final width can be made equal to the size of the atomic sample when trapped in the optical tweezer.

Considering all atom losses throughout the different steps described, it is possible to bring into the final measurement position ~0.4% of the atoms initially trapped in the red MOT. This number can be enhanced, e.g., by improving the vacuum level and increasing the laser power for the optical lattice. Our measurements were made with an initial atom number in the red MOT around $10^6$; this number can be improved by more than one order of magnitude after careful

optimization. Though the transfer efficiency into the optical lattice would be slightly lower at higher atomic density, the number of atoms in the final measurement position can be made high enough to attain a sensitivity to force measurements similar to that reported in [23], where a resolution of 2 ppm on gravity acceleration was demonstrated with only 2 s of measurement time. Moreover, increase in the measurement time by one order of magnitude seems feasible, since very long quantum coherence has been demonstrated with $^{88}$Sr [36]. This would provide a comparable improvement in the sensitivity.

## VII. CONCLUSIONS

In conclusion, we have demonstrated a versatile technique to optically manipulate a sample of ultracold strontium atoms in order to measure atom-surface forces at distances below 10 $\mu$m with high precision. We have characterized the reproducibility of the atom-surface distance at the level of 2 $\mu$m. Further progress in the displacement resolution may be achieved by better focusing the laser beams for the optical tweezer and by mechanical stabilization of the optical setup. In the force detection all spurious effects due to the atomic motion in the elevator, including the lattice modulation caused by the substrate reflectivity, are rejected by measuring the frequency of Bloch oscillations with atoms at rest at a given distance by the test surface. The projected sensitivity of force measurement can be estimated at the level of $10^{-6}$–$10^{-7}$ times the earth's gravity. This will allow precise measurements of position-dependent forces with strong gradients such as Casimir-Polder interaction and to search for hypothetical short-range non-Newtonian gravity.

## ACKNOWLEDGMENTS

This work was supported by LENS, INFN, EU (under Contract No. RII3-CT-2003 506350 and the FINAQS project), ASI, and Ente CRF.

[1] D. M. Harber, J. M. Obrecht, J. M. McGuirk, and E. A. Cornell, Phys. Rev. A **72**, 033610 (2005).
[2] G. Ferrari, N. Poli, F. Sorrentino, and G. M. Tino, Phys. Rev. Lett. **97**, 060402 (2006).
[3] S. Dimopoulos and A. A. Geraci, Phys. Rev. D **68**, 124021 (2003).
[4] I. Carusotto, L. Pitaevskii, S. Stringari, G. Modugno, and M. Inguscio, Phys. Rev. Lett. **95**, 093202 (2005).
[5] H. B. Chan, V. A. Aksyuk, R. N. Kleiman, D. J. Bishop, and F. Capasso, Phys. Rev. Lett. **87**, 211801 (2001).
[6] L. Randall, Science **296**, 5572 (2002).
[7] G. M. Tino, in *A Relativistic Spacetime Odyssey—Proceedings of JH Workshop, Firenze, 2001*, edited by I. Ciufolini, D. Dominici, and L. Lusanna (World Scientific, Singapore, 2003).
[8] J. C. Long, H. W. Chan, A. B. Churnside, E. A. Gulbis, M. C. M. Varney, and J. C. Price, Nature (London) **421**, 922 (2003).
[9] S. J. Smullin, A. A. Geraci, D. M. Weld, J. Chiaverini, S. Holmes, and A. Kapitulnik, Phys. Rev. D **72**, 122001 (2005).
[10] J. Chiaverini, S. J. Smullin, A. A. Geraci, D. M. Weld, and A. Kapitulnik, Phys. Rev. Lett. **90**, 151101 (2003).
[11] G. Bressi, G. Carugno, R. Onofrio, and G. Ruoso, Phys. Rev. Lett. **88**, 041804 (2002).
[12] C. D. Hoyle, D. J. Kapner, B. R. Heckel, E. G. Adelberger, J. H. Gundlach, U. Schmidt, and H. E. Swanson, Phys. Rev. D **70**, 042004 (2004).
[13] R. S. Decca, E. Fischbach, G. L. Klimchitskaya, D. E. Krause, D. López, and V. M. Mostepanenko, Phys. Rev. D **68**, 116003 (2003).
[14] D. M. Weld, J. Xia, B. Cabrera, and A. Kapitulnik, Phys. Rev. D **77**, 062006 (2008).
[15] J. M. Obrecht, R. J. Wild, M. Antezza, L. P. Pitaevskii, S. Stringari, and E. A. Cornell, Phys. Rev. Lett. **98**, 063201 (2007).
[16] B. P. Anderson and M. A. Kasevich, Science **282**, 1686 (1998).
[17] A. Peters, K. Y. Chung, and S. Chu, Nature (London) **400**, 849 (1999).
[18] G. M. Tino, Nucl. Phys. B **113**, 289 (2002).
[19] M. Raizen, C. Salomon, and Q. Niu, Phys. Today **50** (7), 30 (1997).
[20] G. Roati, E. de Mirandes, F. Ferlaino, H. Ott, G. Modugno, and M. Inguscio, Phys. Rev. Lett. **92**, 230402 (2004).
[21] M. Gustavsson, E. Haller, M. J. Mark, J. G. Danzl, G. Rojas-Kopeinig, and H.-C. Nägerl, Phys. Rev. Lett. **100**, 080404 (2008).
[22] M. Fattori, C. D'Errico, G. Roati, M. Zaccanti, M. Jona-Lasinio, M. Modugno, M. Inguscio, and G. Modugno, Phys. Rev. Lett. **100**, 080405 (2008).
[23] V. V. Ivanov, A. Alberti, M. Schioppo, G. Ferrari, M. Artoni, M. L. Chiofalo, and G. M. Tino, Phys. Rev. Lett. **100**, 043602 (2008).
[24] G. Ferrari, R. E. Drullinger, N. Poli, F. Sorrentino, and G. M. Tino, Phys. Rev. A **73**, 023408 (2006).
[25] F. Sorrentino, G. Ferrari, N. Poli, R. E. Drullinger, and G. M. Tino, Mod. Phys. Lett. B **20**, 1287 (2006).
[26] P. K. Rekdal, S. Scheel, P. L. Knight, and E. A. Hinds, Phys. Rev. A **70**, 013811 (2004).
[27] H. Katori, T. Ido, Y. Isoya, and M. Kuwata-Gonokami, Phys. Rev. Lett. **82**, 1116 (1999).
[28] T. H. Loftus, T. Ido, A. D. Ludlow, M. M. Boyd, and J. Ye, Phys. Rev. Lett. **93**, 073003 (2004).
[29] N. Poli, R. E. Drullinger, G. Ferrari, J. Léonard, F. Sorrentino, and G. M. Tino, Phys. Rev. A **71**, 061403(R) (2005).
[30] D. Schrader, S. Kuhr, W. Alt, M. Müller, V. Gomer, and D. Meschede, Appl. Phys. B: Lasers Opt. **73**, 819 (2001).
[31] S. Schmid, G. Thalhammer, K. Winkler, F. Lang, and J. H. Denschlag, New J. Phys. **8**, 159 (2006).
[32] C. F. Bharucha, K. W. Madison, P. R. Morrow, S. R. Wilkinson, B. Sundaram, and M. G. Raizen, Phys. Rev. A **55**, R857 (1997).
[33] E. Lifshits, Sov. Phys. JETP **2**, 73 (1956).

[34] M. Antezza, L. P. Pitaevskii, and S. Stringari, Phys. Rev. Lett. **95**, 113202 (2005).

[35] H. L. Schwartz, T. M. Miller, and B. Bederson, Phys. Rev. A **10**, 1924 (1974).

[36] A. Alberti, V. V. Ivanov, G. M. Tino, and G. Ferrari, e-print arXiv:0803.4069.

[37] T. Meyrath, F. Schreck, J. Hanssen, C.-S. Chuu, and M. Raizen, Opt. Express **13**, 2843 (2005).